nature chemical biology

SUPPLEMENTARY INFORMATION

https://doi.org/10.1038/s41589-018-0209-y

In the format provided by the authors and unedited.

Junction resolving enzymes use multivalency to keep the Holliday junction dynamic

Ruobo Zhou[1,2*], Olivia Yang[3], Anne-Cécile Déclais[4], Hyeonseok Jin[5], Gwang Hyeon Gwon[5], Alasdair D. J. Freeman[4], Yunje Cho[5], David M. J. Lilley[4] and Taekjip Ha[1,3,6,7,8*]

[1]Department of Physics and Center for the Physics of Living Cells, University of Illinois at Urbana-Champaign, Champaign, IL, USA. [2]Department of Chemistry and Chemical Biology, Harvard University, Cambridge, MA, USA. [3]Department of Biophysics and Biophysical Chemistry, Johns Hopkins University, Baltimore, MD, USA. [4]Cancer Research UK Nucleic Acid Structure Research Group, School of Life Sciences, The University of Dundee, Dundee, UK. [5]Department of Life Science, Pohang University of Science and Technology, Pohang, South Korea. [6]Howard Hughes Medical Institute, Baltimore, MD, USA. [7]Department of Biophysics, Johns Hopkins University, Baltimore, MD, USA. [8]Department of Biomedical Engineering, Johns Hopkins University, Baltimore, MD, USA. *e-mail: ruobozhou@fas.harvard.edu; tjha@jhu.edu

SUPPLEMENTARY INFORMATION

Junction resolving enzymes use multivalency to keep the Holliday junction dynamic

Ruobo Zhou[1,2,*], Olivia Yang[3], Anne-Cécile Déclais[4], Hyeonseok Jin[5], Gwang Hyeon Gwon[5], Alasdair D. J. Freeman[4], Yunje Cho[5], David M. J. Lilley[4] and Taekjip Ha[1,3,6,7,8,*]

[1]Department of Physics and Center for the Physics of Living Cells, University of Illinois at Urbana-Champaign, IL, USA

[2]Department of Chemistry and Chemical Biology, Harvard University, Cambridge, MA, USA

[3]Department of Biophysics and Biophysical Chemistry, Baltimore, MD, USA

[4]Cancer Research UK Nucleic Acid Structure Research Group, School of Life Sciences, The University of Dundee, Dundee, U.K.

[5]Department of Life Science, Pohang University of Science and Technology, Pohang, South Korea

[6]Howard Hughes Medical Institute, Baltimore, MD, USA

[7]Department of Biophysics, Johns Hopkins University, Baltimore, MD, USA

[8]Department of Biomedical Engineering, Johns Hopkins University, Baltimore, MD, USA

*Correspondence should be addressed to T.H. (tjha@jhu.edu) or R.Z. (ruobozhou@fas.harvard.edu).

Table of Contents

	DNA only			+hMus81-Eme1			+RuvC		+Endo Δ	+K67A Δ
	J7E	**n-J5m**	**J5m**	**J7E**	**n-J5m**	**J5m**	**J7E**	**J5m**	**J5m**	**J5m**
5 mM EDTA	N.A.	N.A.	0.016±0.012	0.15±0.01 3.5±0.1	0.018±0.021 0.70±0.01	0.041±0.01 0.44±0.02	N.A.	0.089 ±0.005 4.4±0.3	0.095 ±0.008 3.0±0.3	0.096 ±0.005 2.2±0.5
1 mM Ca^{2+}	0.026±0.04	0.026±0.005	0.073±0.002	0.22±0.01 1.5±0.1	0.061±0.005 0.74±0.03	0.059±0.007 0.53±0.07	N.A.	0.29±0.02 4.2±0.1	N.A.	N.A.
10 mM Ca^{2+}	0.20±0.01	0.17±0.01	0.53±0.07	0.20 ±0.01 0.56±0.05	0.061±0.005 0.48±0.05	0.084±0.018 1.0±0.1	0.16±0.01 3.0±0.1	0.21±0.01 4.2±0.1	N.A.	N.A.
1 mM Mg^{2+}	N.A.	N.A.	0.095±0.002	N.A.	N.A.	0.072 ±0.018 0.52±0.02	N.A.	0.13±0.01 5.3±0.2	N.A.	N.A.

Supplementary Table 1: The time components of the Holliday junction dynamics obtained from cross-correlation analysis (unit: sec). The cross-correlation functions of I_D and I_A for bare J7E, J5m and n-J5m can be fit by single exponential function, whereas the cross-correlations of I_D and I_A for resolving-enzyme-bound J7E, J5m and n-J5m can be fit by bi-exponential function. It indicates that the HJ dynamics can be described by a single time component without a protein bound, but can be described by two time components differing by more than one order of magnitude with the protein bound. The shorter time component is likely related to the rate of conformer exchange or branch migration dynamics in the PD mode, and the longer time component is likely related to the transition rates between the PD mode and the fully bound state. Means ± s.e.m are indicated (n = 1,000 HJ molecules).

DNA constructs	DNA sequences
Junction 7 (J7)	5’ - CCTCCCTAGCAAGCCGCTGCTACGG - 3’ 5’ - /Cy3/CCGTAGCAGCGCGAGCGGTGGG - 3’ 5’- /biotin/CCCACCGCTCGGCTCAACTGGG - 3’ 5’- CCCACCGCTCGGCTCAACTGGG - 3’ 5’ - CCCAGTTGAGCGCTTGCTAGG G/Cy5/ - 3’
J7E	5’ - CGTGCATGTCCCTAGCAAGCCGCTGCTACGGATCCTTGGC - 3’ 5’ - GCCAAGG/Cy3/ATCCGTAGCAGCGCGAGCGGTGGGCGAACGTCT - 3’ 5’ - /biotin/AGACGTTCGCCCACCGCTCGGCTCAACTGGGACCGTTTCG - 3’ 5’ - CGAAACGGTCCCAGTTGAGCGCTTGCTAGGGACA/Cy5/TGCACG - 3’
Unlabeled J7	5’ - CCTCCCTAGCAAGCCGCTGCTACGG - 3’ 5’ - CCCACCGCTCGGCTCAACTGGG - 3’ 5’ - CCGTAGCAGCGCGAGCGGTGGG - 3’ 5’ - CCCAGTTGAGCGCTTGCTAGGG - 3’
22-bp double-stranded (ds)DNA	5’ - CCCACCGCTCGGCTCAACTGGG - 3’ 5’ - CCCAGTTGAGCCGAGCGG TGGG - 3’
Junction 3 (J3)	5’ - TCCGTCCTAGCAAGGGGCTGCTACCGGAAG - 3’ 5’ - CTTCCGGTAGCAGCCTGAGCGGTGGTTGAA - 3’ 5’ - TTCAACCACCGCTCAACTCAACTGCAGTCT - 3’ 5’ - AGACTGCAGTTGAGTCCTTGCTAGGACGGA - 3’
RCUNC1	5’ - TCCGTCCTAGCAATGGTGTGCTACCGGAAG - 3’ 5’ - CTTCCGGTAGCACACAATCCGGTGGT/Cy5/TGAATTCCT - 3’ 5’ - /biotin/AGGAATTCAACCACCGGATTCAGGAACTGCAGTCTAGACT - 3’ 5’ - AGTCTAGAC/Cy3/TGCAGTTCCTGCATTGCTAGGACGGA - 3’
J0m	5’ - /biotin/TCTTTTGATAAGCTTGCAAGCATACTAAACTCGTAATTTCCGGTTAGGT - 3’ 5’ – ACCTAACCGGAAATTACGAGTTATCGATGCATGCAAGCTTCACA - 3’ 5’ - TGTGAAGCTTGCA/iAmMC6T/GCATCGATCTAATACGTGAGGCCTAGGATC - 3’ 5’ - GATCCTAGGCCTCACGTATTAGTAGTATGC/iAmMC6T/TGCAAGCTTATCA - 3’
J5m	5’ - /biotin/TCTTTTGATAAGCTTGCAAGCATAGATATCTCGTAATTTCCGGTT AGGT - 3’ 5’ – ACCTAACCGGAAATTACGAGATATCGATGCATGCAAGCTTCACA - 3’ 5’ - TGTGAAGCTTGCA/iAmMC6T/GCATCGATATAATACGTGAGGCCTAGGATC - 3’ 5’ - GATCCTAGGCCTCACGTATTATATCTATGC/iAmMC6T/TGCAAGCTTATCA - 3’

Nicked-J5m (n-J5m)	5’ - /biotin/TCTTTTGATAAGCTTGCAAGCATAGATATCTCGTAATTTCCGGTT AGGT - 3’ 5’ - ACCTAACCGGAAATTACGAGAT - 3’ 5’ - /Phos/ATCGATGCATGCAAGCTTCACA - 3’ 5’ - TGTGAAGCTTGCA/iAmMC6T/GCATCGATATAATACGTGAG GCCTAGGA TC - 3’ 5’ - GATCCTAGGCCTCACGTATTATATCTATGC/iAmMC6T/TGCA AGCTTATCA - 3’

Supplementary Table 2: DNA sequences for annealing the Holliday junction and double-stranded DNA constructs. The amine-modified thymine (/iAmMC6T/) shown in the sequence enables the oligonucleotides to be labeled with the monofunctional NHS ester form of Cy3 or Cy5 dyes (GE Healthcare). Otherwise, Cy3 or Cy5 dye was attached directly to the DNA backbone using phosphoramidite chemistry. /biotin/ and /Phos/ represents the biotin and phosphorylation modification respectively.

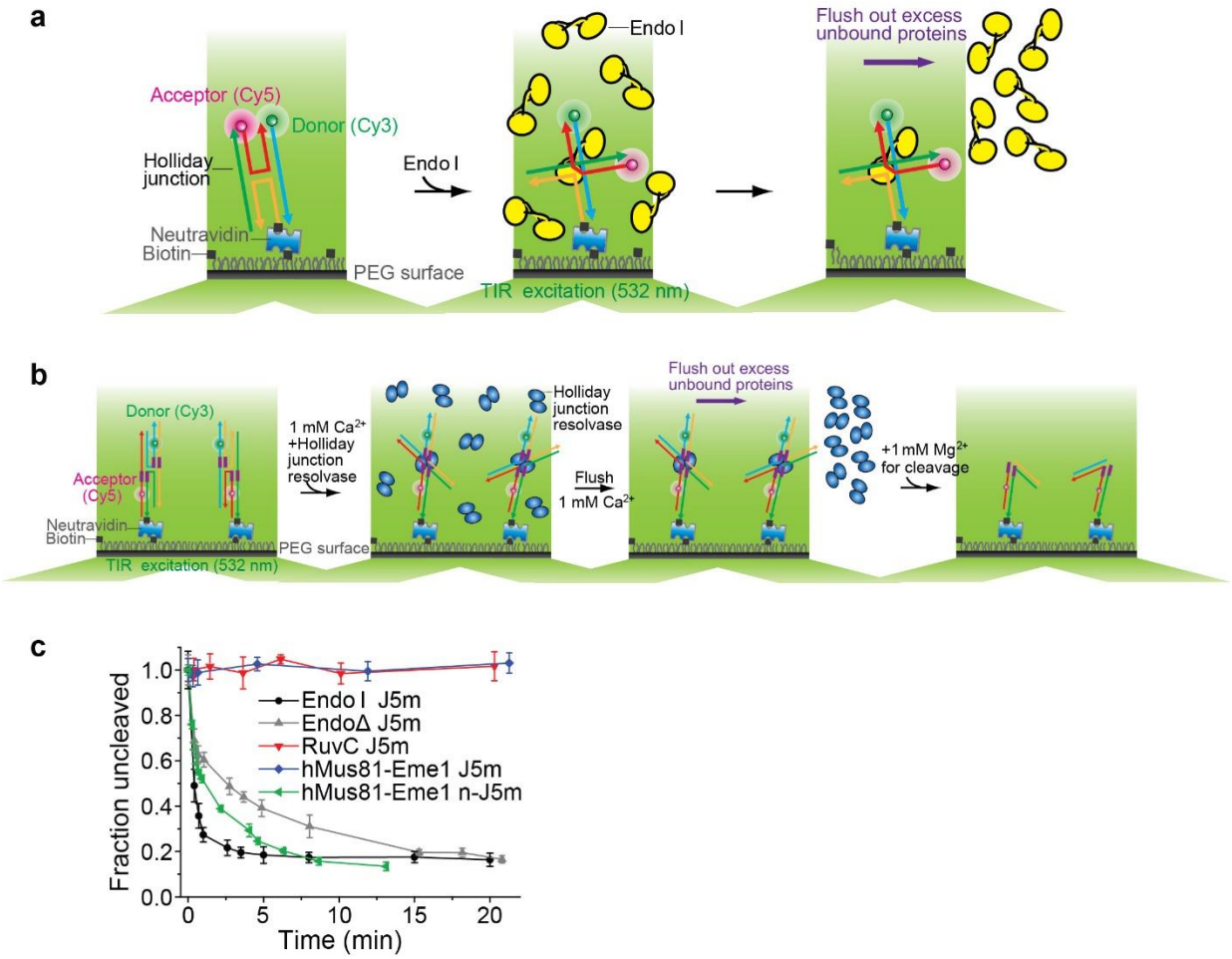

Supplementary Figure 1: Experimental schemes for our single molecule analysis of resolving-enzyme-bound Holliday junction molecules. a, Experimental scheme for monitoring the dynamics of individual resolving-enzyme-bound Holliday junction molecules. After incubating Endo I with surface-immobilized junctions, unbound proteins were flushed out before data acquisition. **b,** Experimental scheme for the Holliday junction resolving enzyme cleavage assay under single molecule conditions. **c,** The uncleaved HJ fraction as a function of reaction time. Data are means ± s.e.m. of $N = 3$ independent experiments.

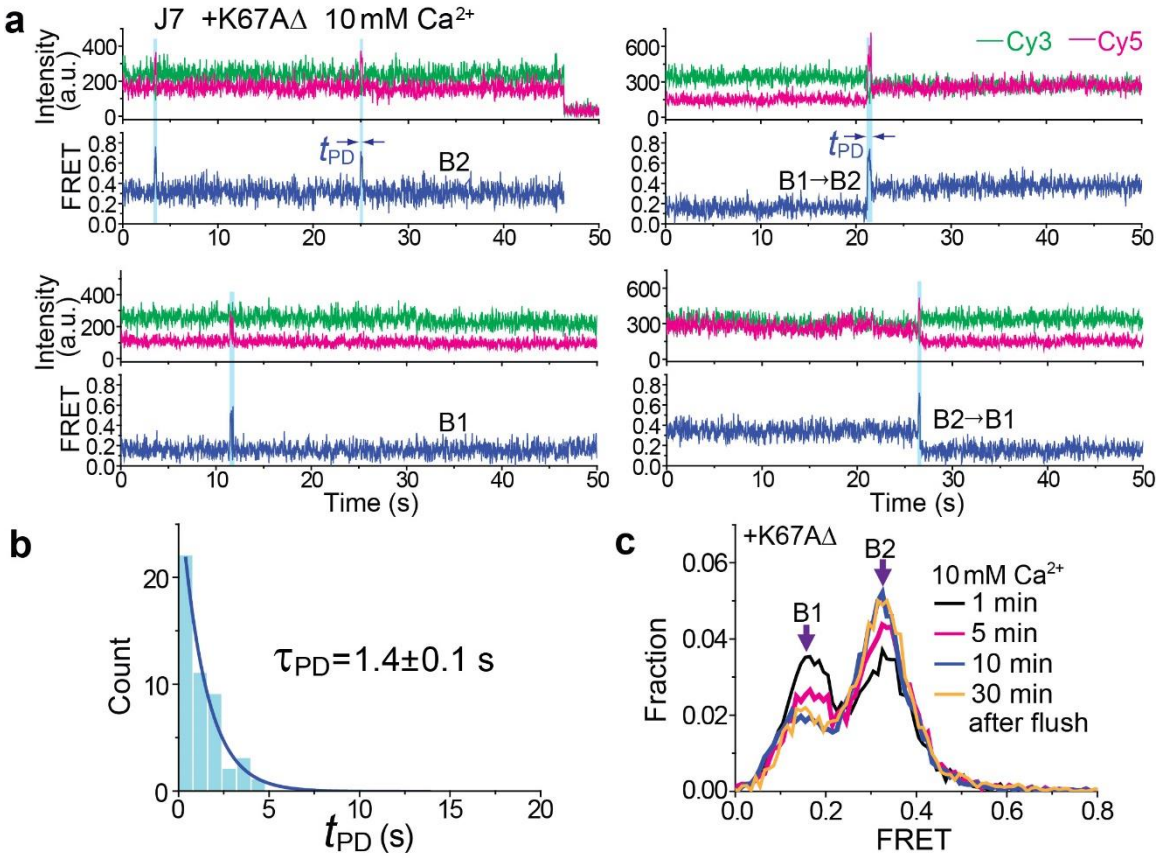

Supplementary Figure 2: Conformer exchange between B1 and B2 for Endo I-bound J7 through the partially dissociated (PD) intermediate. a, Representative single molecule time traces of K67AΔ-bound J7. Partial dissociation of K67AΔ from J7 (blue-shaded regions) was observed as brief excursions from $E_{0.35}$ (**B2**) to $E_{0.6}$ (**U2**), or from $E_{0.15}$ (**B1**) *to* $E_{0.6}$ (**U2**). Although partial dissociation did not always lead to conformer exchange (left), it was often observed as an intermediate state for exchange between **B1** and **B2** (right). The **PD** intermediate here is too short-lived to exhibit multiple rounds of **U1↔U2** transitions as shown later for RuvC-bound HJs (Figure 3c) and GEN1-bound HJs (Figure 4b). **b, PD** dwell time (t_{PD}) histogram for K67AΔ-bound J7 fit by a single exponential function. Mean ± s.e.m is indicated (n = 50 dwell times).**c,** E_{FRET} histograms of K67AΔ-bound J7 obtained at 10 mM Ca^{2+} at different time points after flushing out excess unbound proteins, indicating the **B1/ B2** population equilibrium took ~ 10 min to reach via slow conformer exchange observed in **a**.

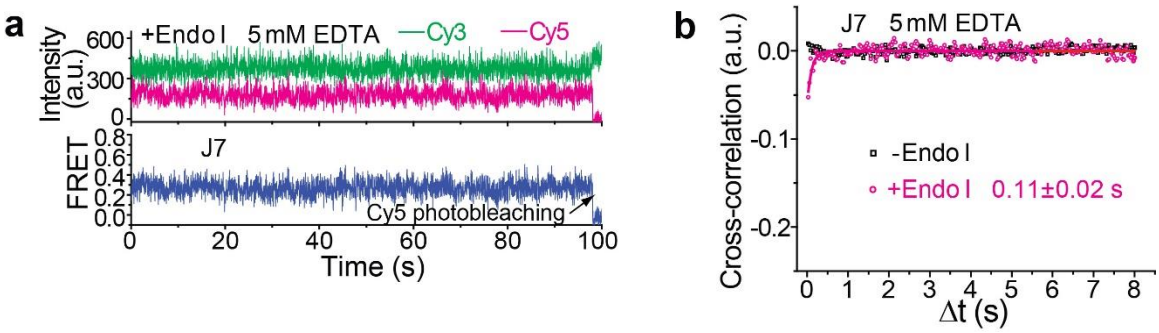

Supplementary Figure 3: Dynamics of Endo I-bound HJs observed in EDTA. a, Single molecule time traces of Endo I-bound J7 showing E_{FRET} fluctuations without Ca^{2+} (in 5 mM EDTA). **b,** Cross-correlation of I_D and I_A for bare and Endo I-bound J7 in 5 mM EDTA. The cross-correlation was fit to a single exponential function (solid line) for Endo-bound J7. Mean ± s.e.m is indicated (n = 1,000 HJ molecules).

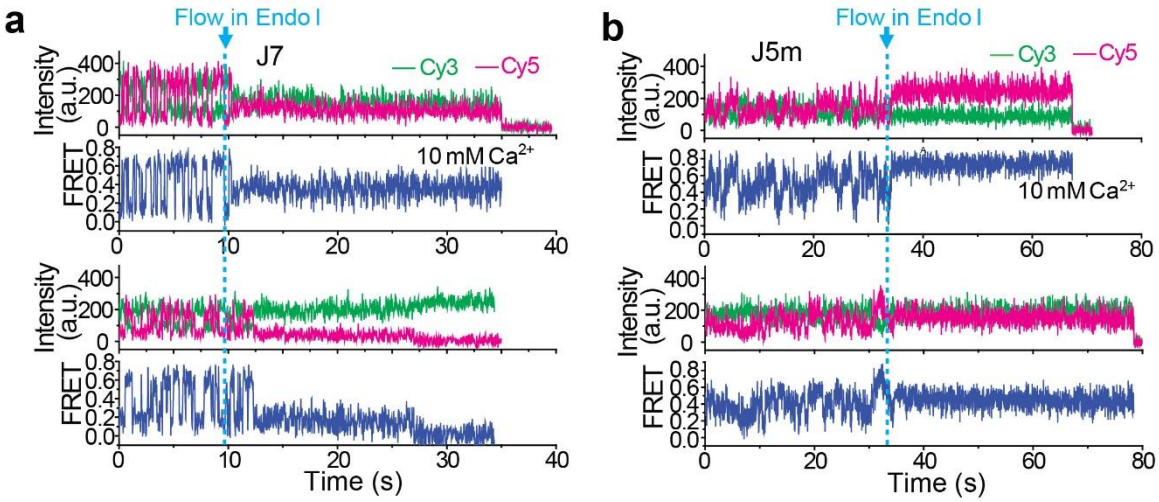

Supplementary Figure 4: Endo I binding events captured by flow experiments. a, Single molecule time traces of J7 showing an Endo I binding event. 10 nM Endo I were added at the time the blue dashed line indicates. J7 flipped back and forth rapidly between **U1** ($E_{0.15}$, i.e., E_{FRET}=0.15) and **U2** ($E_{0.6}$) until Endo I was bound, which stabilized J7 to either **B1** ($E_{0.15}$) or **B2** ($E_{0.35}$). **b,** Single molecule time traces of J5m showing an Endo I binding event. 10 nM Endo I were added at the time the blue dashed line indicates. Endo I binding largely stabilized J5m to a single E_{FRET} state but the stabilized E_{FRET} value could differ widely among different molecules, likely due to the freezing/capture of an instantaneous branch point upon Endo I binding.

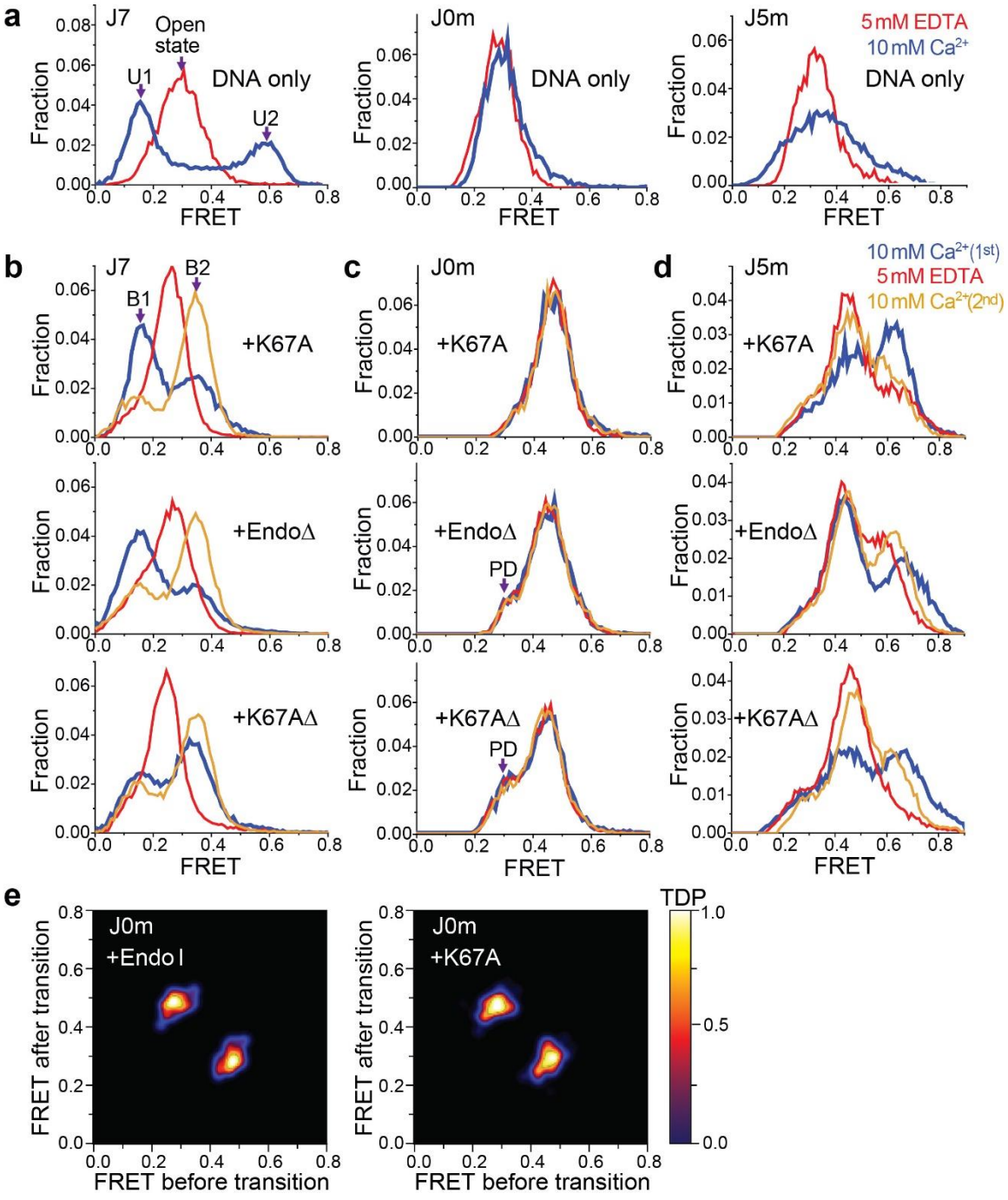

Supplementary Figure 5: Ca^{2+}-EDTA-Ca^{2+} buffer exchange experiments for Endo I-bound HJs and TDP analysis of Endo-I bound J0m. a, E_{FRET} histograms of bare HJs (J7, J0m and J5m) obtained at 5 mM EDTA (red) and 10 mM Ca^{2+} (blue). Replicated from Figures 1g and 2d for comparison with E_{FRET} histograms of bound HJs. **b,** E_{FRET} histograms obtained before (blue), during (red), and after (yellow) the EDTA pulse for J7 associated with the three Endo I mutants. Endo I binding induced two major conformers

(**B1** and **B2**) and Endo I did not dissociate throughout the EDTA pulse experiment. The relative ratio of HJ fractions adopting **B1** and **B2** changed when Ca^{2+} was reintroduced. **c,** E_{FRET} histograms obtained before (blue), during (red), and after (yellow) the EDTA pulse for mutant-bound J0m, showing one dominant peak at $E_{0.45}$ (the fully bound state) and a minor peak at $E_{0.3}$ (the **PD** state). **d,** E_{FRET} histograms obtained before (blue), during (red), and after (yellow) the EDTA pulse for mutant-bound J5m, showing a broad distribution with multiple peaks which correspond to the six possible branchpoint positions. **e,** Transition density plots (TDPs) where the occurrences of transitions between distinct E_{FRET} states were plotted against two-dimensional E_{FRET} (before) and E_{FRET} (after) plane, for wild type Endo I and K67A, showing transitions between $E_{0.3}$ and $E_{0.45}$ states, although the $E_{0.3}$ state was not well detected in their E_{FRET} histograms (**c** and Figure 2d).

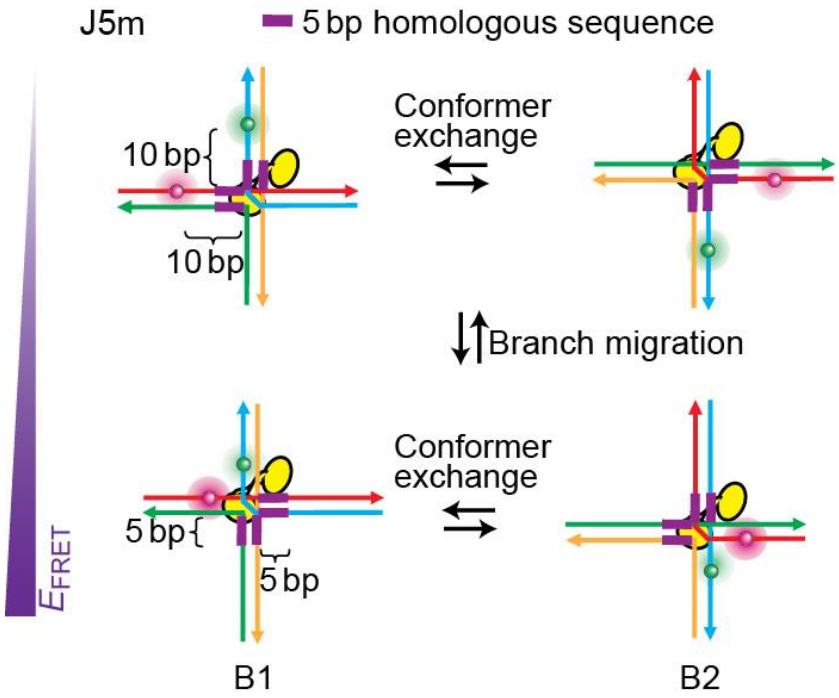

Supplementary Figure 6: Schematic of Endo I-bound J5m. The branch migration of Endo I-bound J5m leads to the E_{FRET} changes, whereas the conformer exchange of Endo I-bound J5m does not result in any change in E_{FRET}.

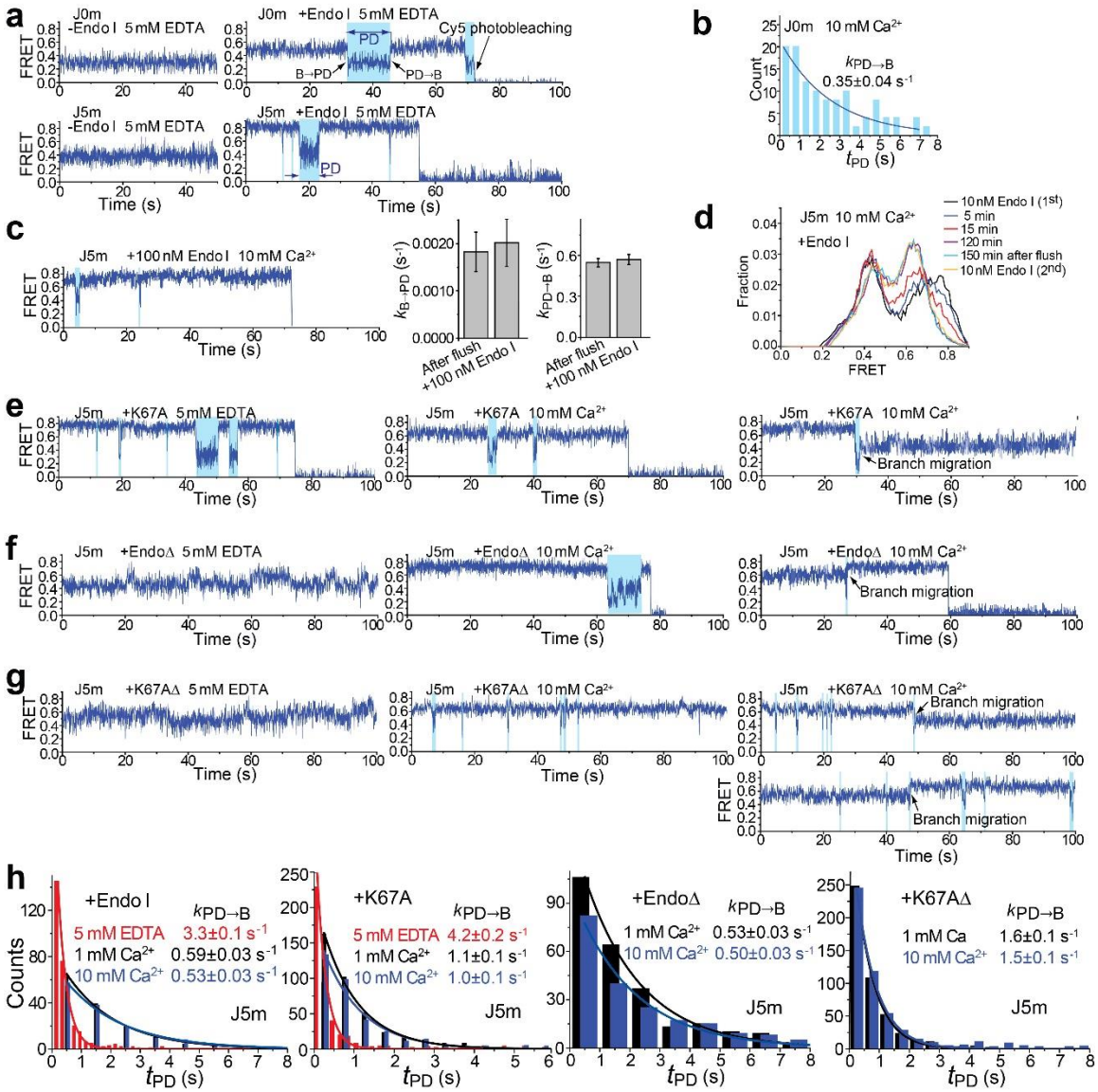

Supplementary Figure 7: Partial dissociation of Endo I mutants permits branch migration of J5m. a, smFRET-time traces of bare and Endo-bound J0m (top) and J5m (bottom) in 5 mM EDTA. The **PD** state of Endo I was observed as a transient drop of a steady E_{FRET} state (the fully bound state) to an E_{FRET} value that resembles the bare HJ. **b,** Dwell time histogram of **PD** for Endo I-bound J0m. Mean ± s.e.m is indicated (n = 105 dwell times). The solid line is the fit to a single exponential function. **c,** Left: smFRET-time trace of Endo I-bound J5m in the presence of 100 nM Endo I. Right: $k_{\mathbf{B\rightarrow PD}}$ and $k_{\mathbf{PD\rightarrow B}}$ obtained for Endo I-bound J5m in the flush condition or in 100 nM Endo I. Data are means ± s.e.m. of n = 1,000 HJ molecules. Error bars represent bootstrap estimates of s.e.m.. **d,** smFRET histograms of Endo I-bound J5m obtained at 10 mM Ca^{2+} at different

time points after flushing out unbound proteins, and after a second addition of protein. **e-g,** smFRET-time traces of K67A (**e**), EndoΔ (**f**), or K67AΔ (**g**) bound J5m, obtained in 5 mM EDTA or in 10 mM Ca^{2+}. Black arrows represent branch migration events which occurred immediately following a visit to the **PD** intermediate. **h,** Dwell time (t_{PD}) histograms for Endo I-bound J5m fit by single exponential function (solid lines). Means ± s.e.m are indicated (n = 1,000 HJ molecules).

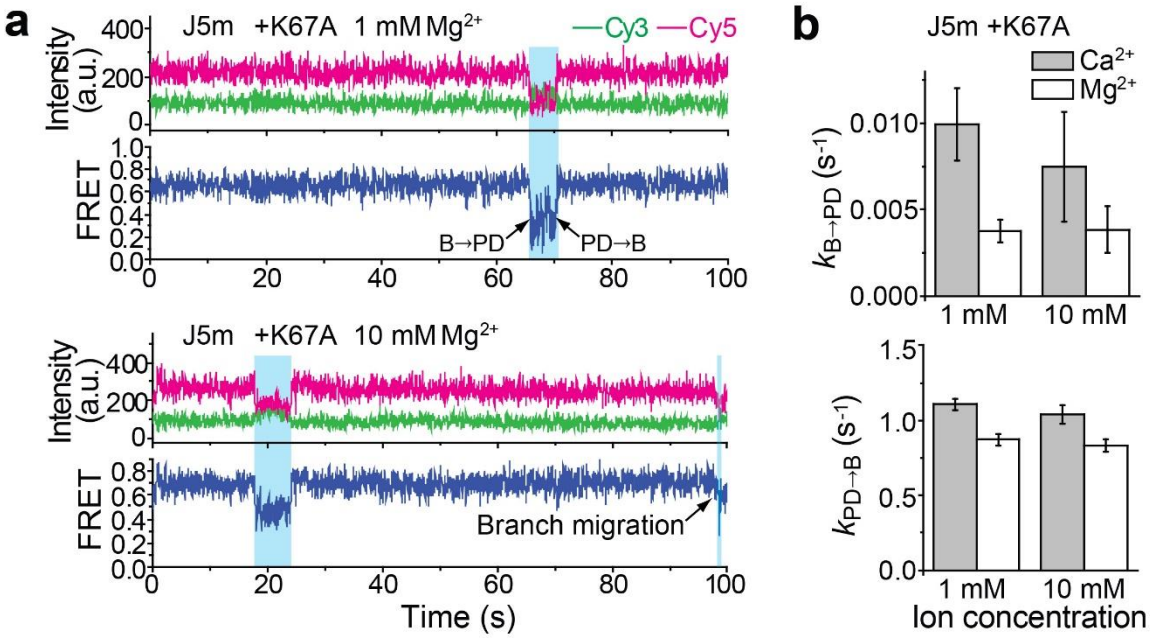

Supplementary Figure 8: Partial dissociation observed in Mg^{2+} for J5m bound by the catalytically-impaired Endo I mutant K67A. a, single molecule time traces of K67A-bound J5m in 1 mM and 10 mM Mg^{2+} (flush condition). **b,** Comparison of $k_{\mathbf{B\rightarrow PD}}$ and $k_{\mathbf{PD\rightarrow B}}$ of K67A-bound J5m obtained in Mg^{2+} with those obtained in Ca^{2+}. Data are means ± s.e.m. of n = 1,000 HJ molecules. Error bars represent bootstrap estimates of s.e.m..

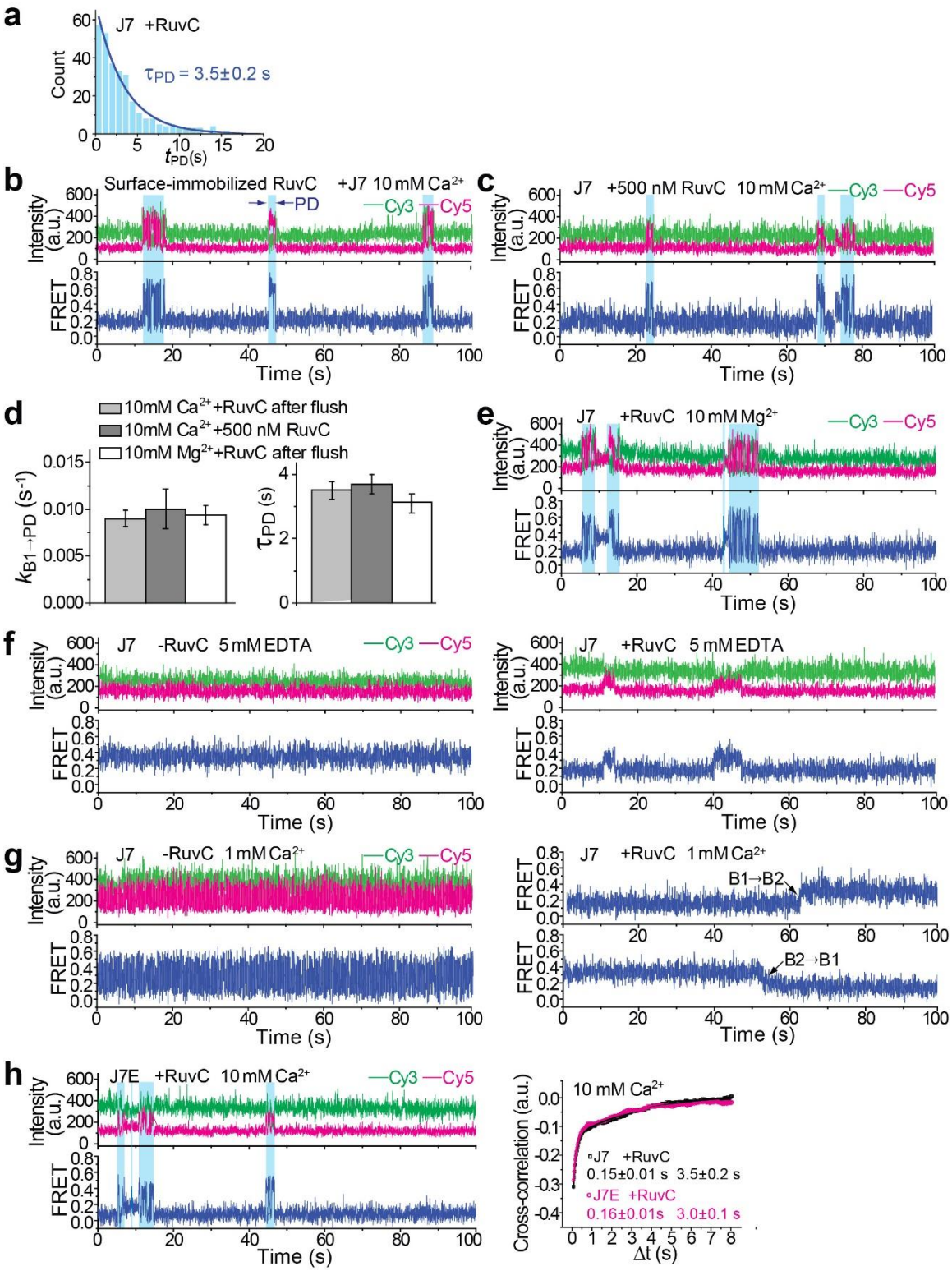

Supplementary Figure 9: RuvC binding to HJs permits conformer exchange through PD at various ionic conditions. a, Histogram of the dwell times of PD (t_{PD}) for RuvC-bound J7. The solid line is the fit to a single exponential function. Mean ± s.e.m is

indicated (n = 286 dwell times). **b,** Single molecule time traces of RuvC-bound J7 at 10 mM Ca^{2+} in a flipped experimental scheme where RuvC, instead of J7, was immobilized in the sample chamber and unbound excess J7 molecules were flushed out. In this experiment, full dissociation followed by binding of another J7 molecule would lead to a transient loss of fluorescence rather than the observed rapid exchange between **U1** and **U2**. **c,** Single molecule time traces of RuvC-bound J7 at 10 mM Ca^{2+} obtained in the presence of 500 nM RuvC. **d,** Comparison of $k_{\mathbf{B\rightarrow PD}}$ and τ_{PD} of RuvC-bound J7 obtained under the three indicated conditions. Data are means ± s.e.m. of n = 1,000 HJ molecules. Error bars represent bootstrap estimates of s.e.m.. **e,** Single molecule time traces of RuvC-bound J7 obtained at 10 mM Mg^{2+} (flush condition). **f and g,** Single molecule time traces of bare (left) and RuvC-bound (right) J7 obtained at 5 mM EDTA (**f**) or 1 mM Ca^{2+} (**g**). **h,** Single molecule time traces (left) and cross-correlation functions of I_D and I_A (right) for RuvC-bound J7E obtained at 10 mM Ca^{2+}. Means ± s.e.m are indicated (n = 1,000 HJ molecules). Cross-correlation analysis suggests the rates of HJ dynamics detected from RuvC-bound J7 and RuvC-bound J7E show no significant difference.

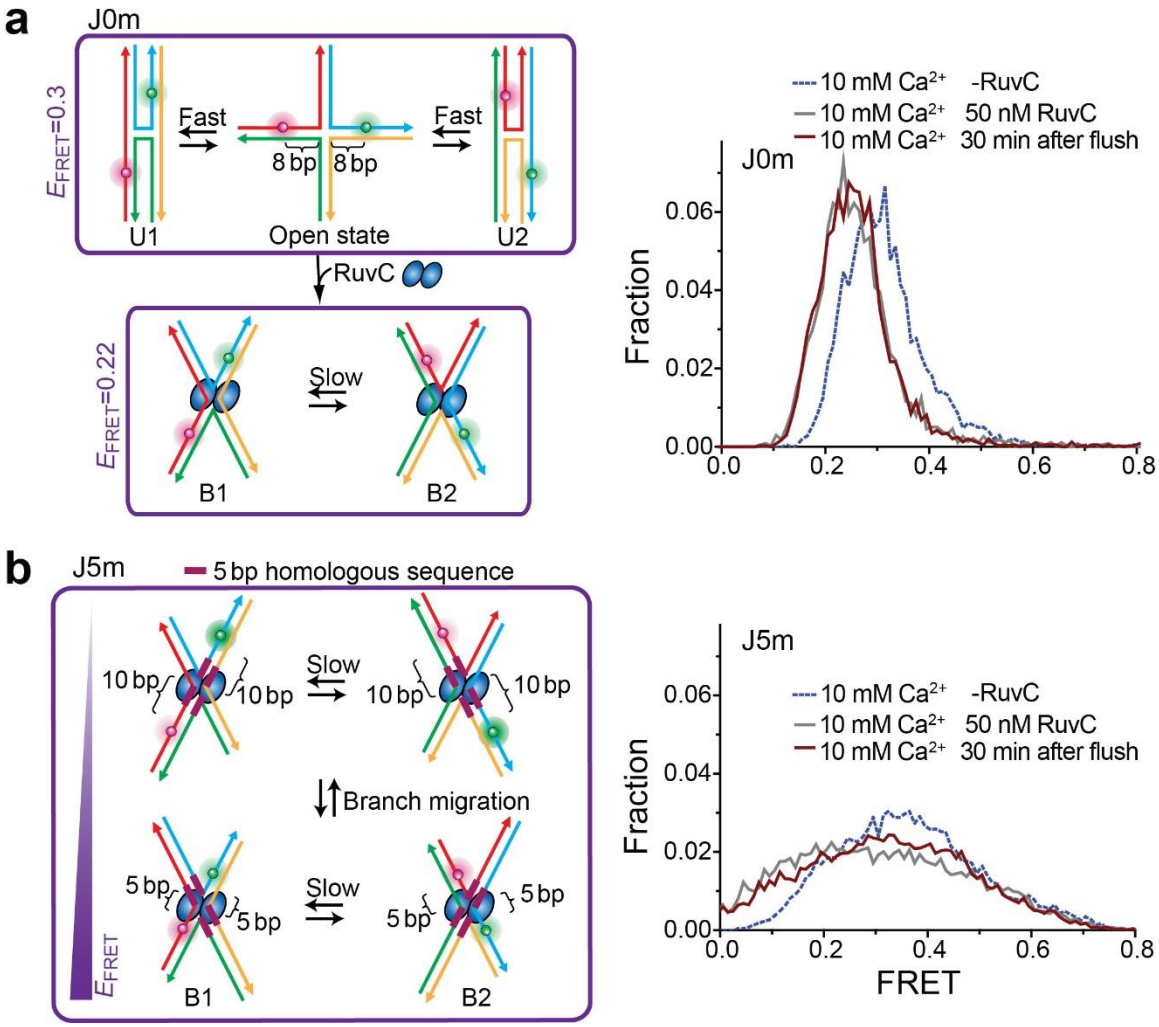

Supplementary Figure 10: RuvC binding to J0m and J5m. a, Schematic of HJ structural dynamics (left) and E_{FRET} histograms of J0m before and after RuvC binding, obtained at 10 mM Ca^{2+} (right). **b,** Schematic of HJ structural dynamics for RuvC-bound J5m (left) and E_{FRET} histograms of J5m before and after RuvC binding, obtained at 10 mM Ca^{2+} (right).

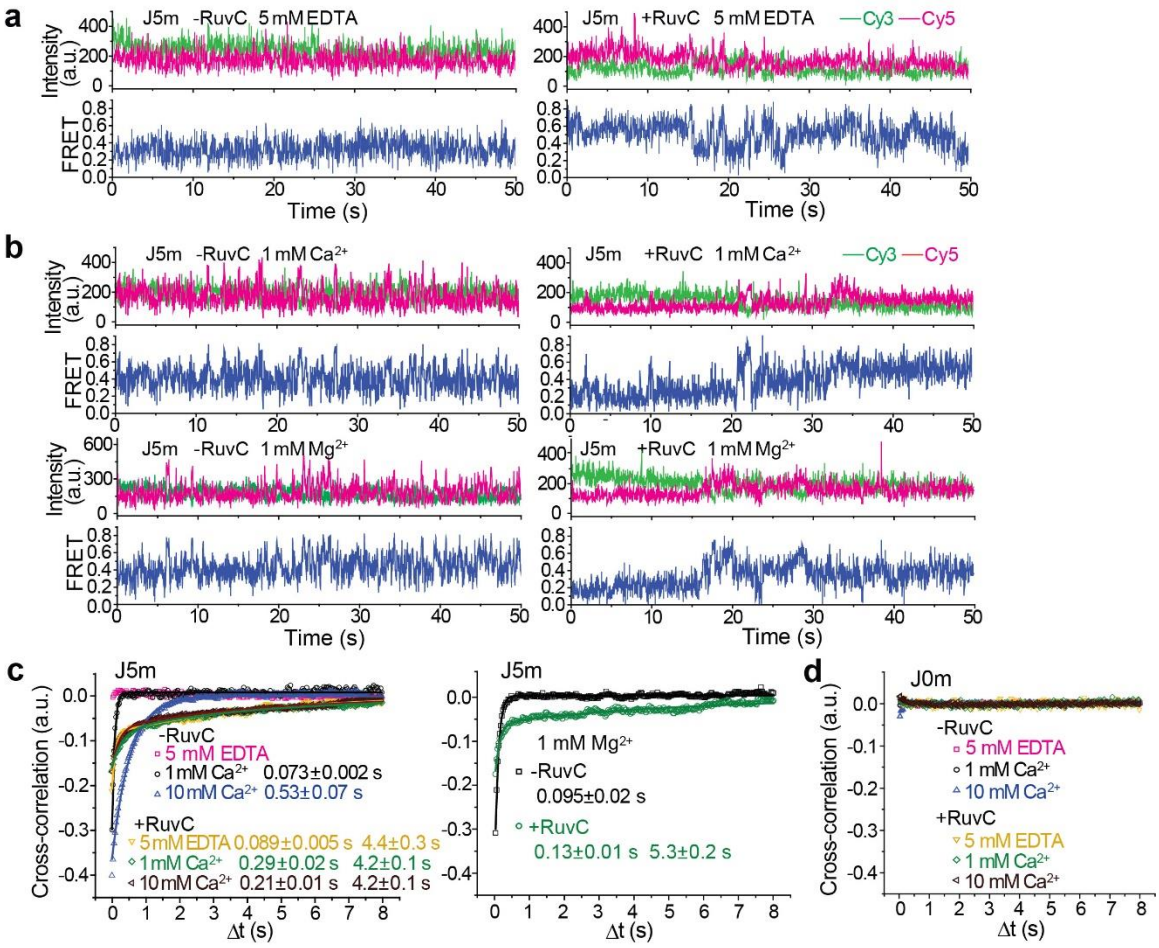

Supplementary Figure 11: RuvC binding to HJs permits branch migration through PD at various ionic conditions. a, Single molecule time traces of bare (left) and RuvC-bound (right) J5m obtained at 5 mM EDTA. **b,** Single molecule time traces of bare (left) and RuvC-bound (right) J5m obtained at 1 mM Ca^{2+} (top) or 1 mM Mg^{2+} (bottom). **c,** Cross-correlation functions of I_D and I_A for bare and RuvC-bound J5m at 0, 1 and 10 mM Ca^{2+} (left), or at 1 mM Mg^{2+} (right). Cross-correlation functions for bare J5m can be fit to single exponential function, whereas those for RuvC-bound J5m can be fit to a bi-exponential function. Means ± s.e.m are indicated (n = 1,000 HJ molecules). **d,** Cross-correlation functions of I_D and I_A for bare and RuvC-bound J0m at 0, 1 and 10 mM Ca^{2+}, as negative controls for those obtained with J5m. No significant anti-correlation was observed between I_D and I_A for J0m.

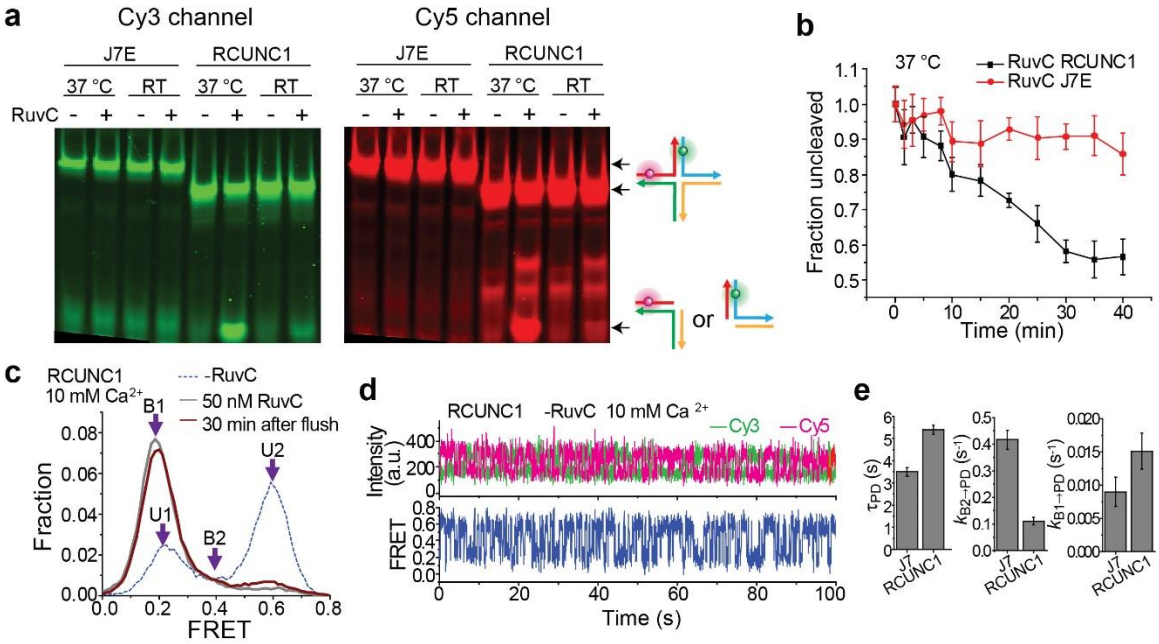

Supplementary Figure 12: RuvC cleavage reaction on a HJ construct containing one RuvC cleavage site (RCUNC1). a and b, Gel retardation assay (**a**) and single molecule assay (**b**) showing the RuvC cleavage was detectable for RCUNC1 but not for J7E. **c,** E_{FRET} histograms of bare and RuvC-bound RCUNC1 obtained at 10 mM Ca^{2+}. Data are means ± s.e.m. of $N = 3$ independent experiments. **d,** Single molecule time traces of bare RCUNC1 showing the rapid two state (**U1** and **U2**) transitions as also observed for bare J7 and J7E. **e,** Comparison of τ_{PD}, $k_{B1\rightarrow PD}$ and $k_{B2\rightarrow PD}$ between RuvC-bound J7 and RCUNC1 at 10 mM Ca^{2+}. Data are means ± s.e.m. of $n = 1{,}000$ HJ molecules. Error bars represent bootstrap estimates of s.e.m..

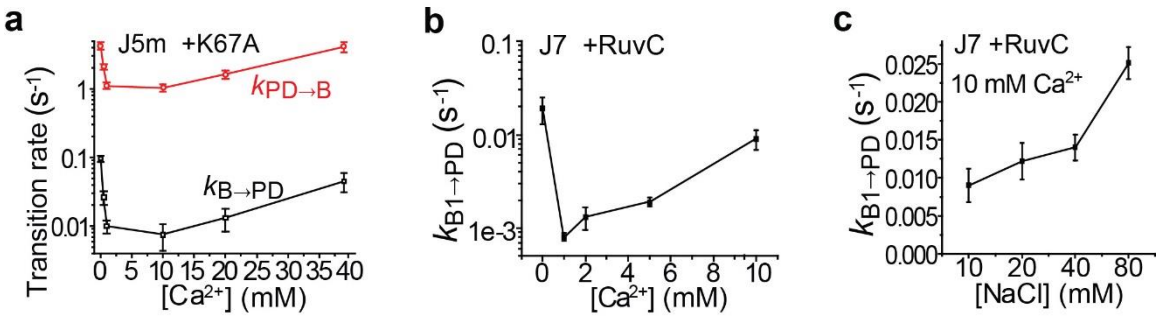

Supplementary Figure 13: Effect of ionic strength on the dynamics of resolving-enzyme-bound Holliday junction. a, [Ca^{2+}] dependence of $k_{\mathbf{B→PD}}$ and $k_{\mathbf{PD→B}}$ obtained for K67A-bound J5m. **b,** [Ca^{2+}] dependence of $k_{\mathbf{B1→PD}}$ obtained for RuvC-bound J7. **c,** [Na^{+}] dependence of $k_{\mathbf{B1→PD}}$ determined for RuvC-bound J7 at 10 mM Ca^{2+}. **a, b, c,** Data are means ± s.e.m. of n = 1,000 HJ molecules. Error bars represent bootstrap estimates of s.e.m..

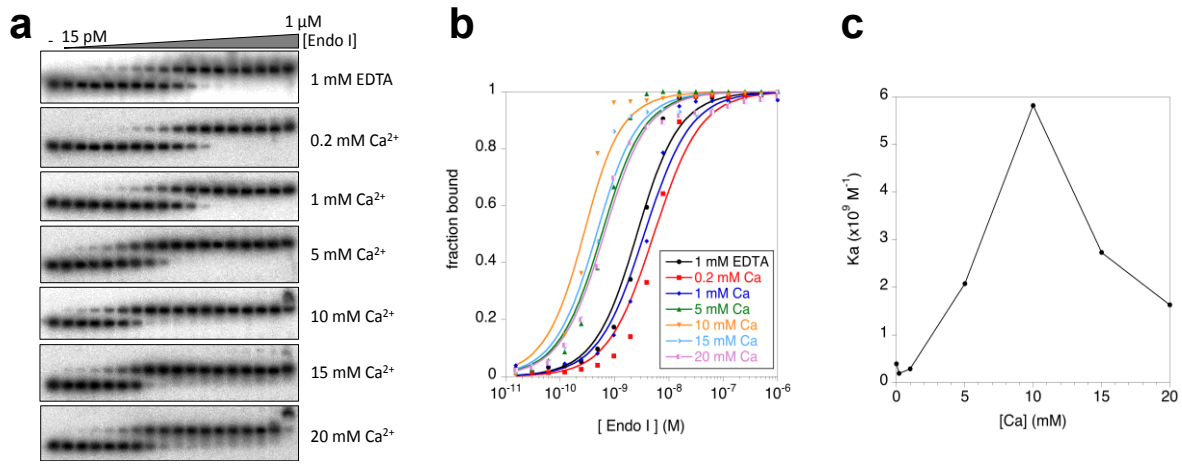

Supplementary Figure 14: Binding affinity of Endo I as a function of [Ca^{2+}]. a, Gel retardation assay. 5′-^{32}P-labelled four-way DNA junction J3 was incubated with increasing amounts of an Endo I variant (EndoΔ11) lacking the unstructured N-terminal tail of 11 amino acids (from 15.3 pM to 1 µM) in the presence of either EDTA or various amounts of $CaCl_2$, and the complexes were separated from the free junction by electrophoresis in a native polyacrylamide gel containing the same concentrations of EDTA or $CaCl_2$. **b,** Binding isotherms obtained by plotting the fraction of bound junction as a function of protein dimer concentration and fitting the data to a two-state model. **c,** Binding affinity coefficients as a function of Ca^{2+} concentration. The zero point represents the 1 mM EDTA condition.

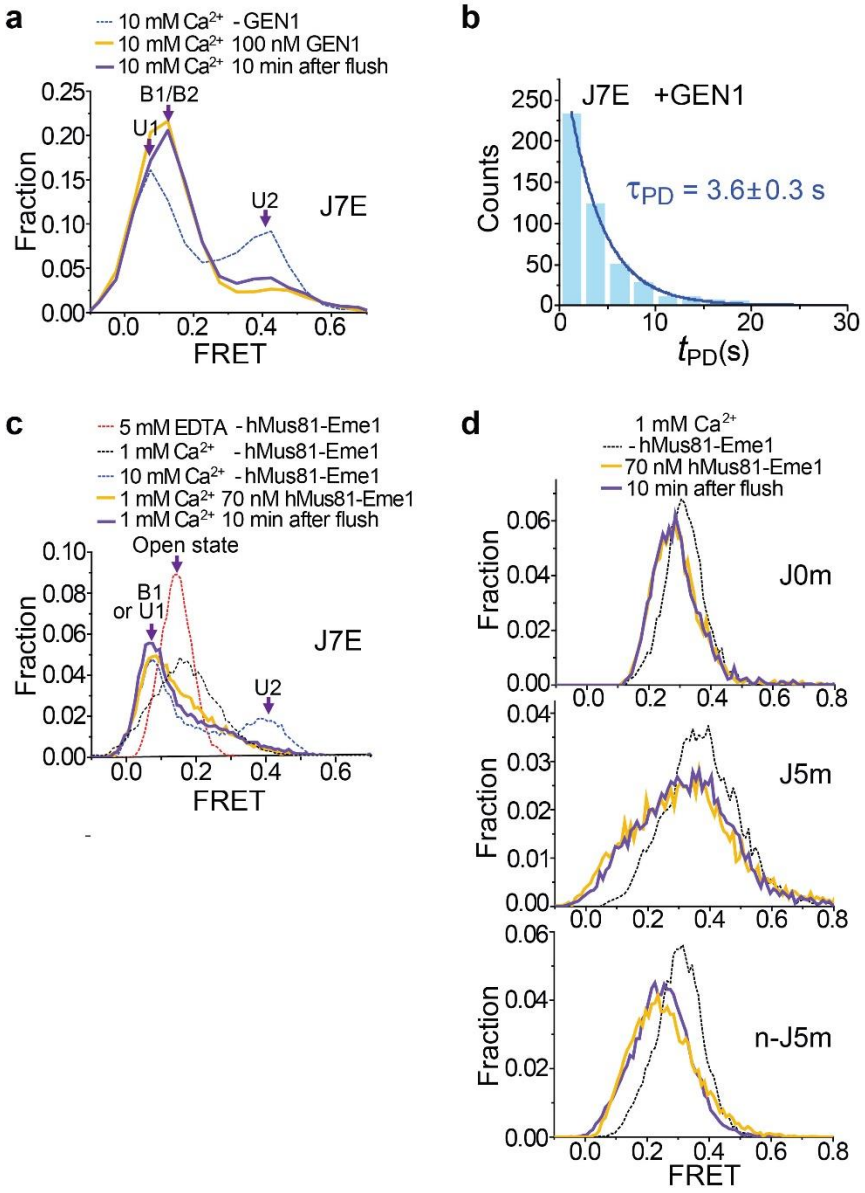

Supplementary Figure 15: GEN1 binding to J7E and hMus81-Eme1 binding to J7E, J0m, J5m and n-J5m. a, E_{FRET} histograms of bare and GEN1-bound J7E obtained at 10 mM Ca^{2+}. **b,** Histogram of the dwell times of PD (t_{PD}) for GEN1-bound J7E. The solid line is the fit to a single exponential function. Mean ± s.e.m is indicated (n = 452 dwell times). **c,** E_{FRET} histograms of bare J7E obtained at 5 mM EDTA, 1 mM Ca^{2+}, or 10 mM Ca^{2+}, and E_{FRET} histograms of hMus81-Eme1-bound J7E, obtained before and after flushing unbound proteins at 1 mM Ca^{2+}. **d,** E_{FRET} histograms of bare and hMus81-Eme1-bound J0m, J5m and n-J5m, obtained at 1 mM Ca^{2+}.

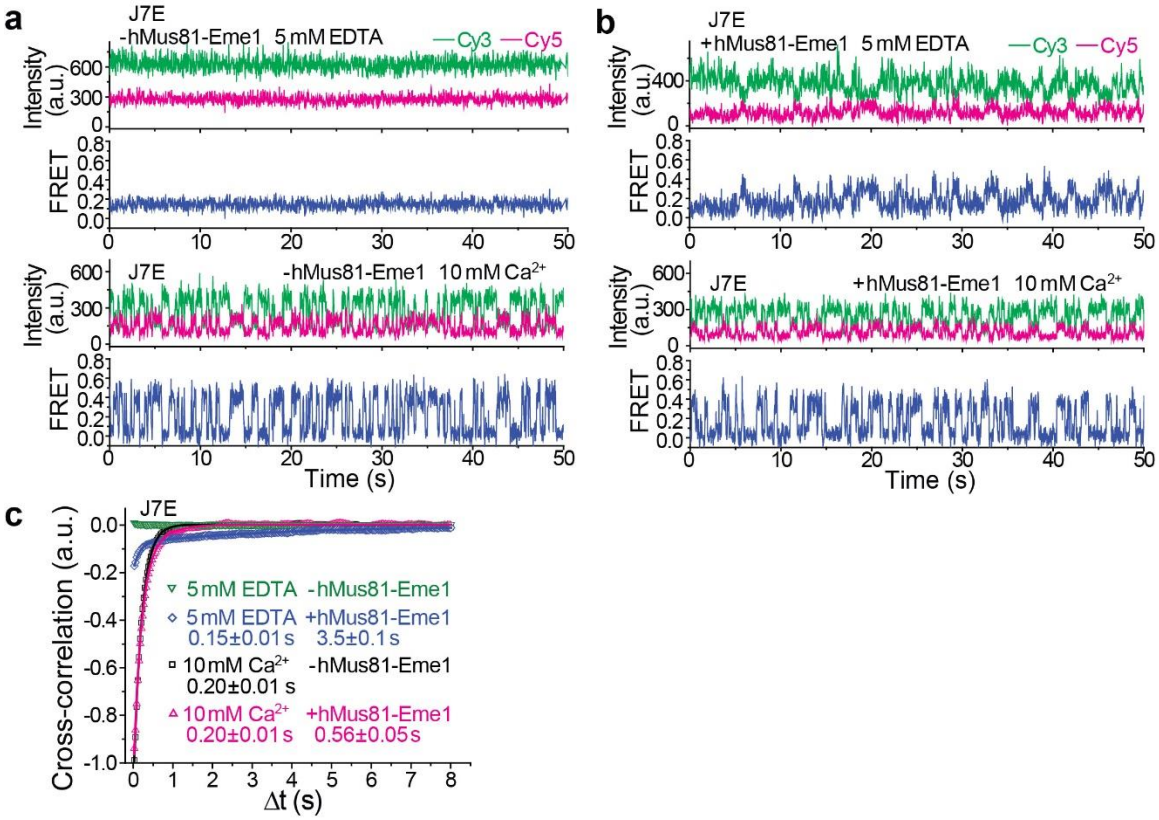

Supplementary Figure 16: hMus81-Eme1 binding to J7E permits conformer exchange between B1 and B2. a and b, Single molecule time traces of bare (**a**) and hMus81-Eme1-bound (**b**) J7E, obtained at 5 mM EDTA or 10 mM Ca^{2+}. The conformer exchange between **B1** and **B2** was observed even with hMus81-Eme1 bound. **c,** Cross-correlation functions of I_D and I_A for bare and hMus81-Eme1-bound J7E, obtained at 5 mM EDTA or 10 mM Ca^{2+}. Cross-correlations for bare J5m can be fit by a single exponential function, while those for hMus81-Eme1-bound J7E can be fit by a bi-exponential function., indicating that the HJ dynamics can be described by a single time component without hMus81-Eme1 bound and two time components with hMus81-Eme1 bound. Means ± s.e.m are indicated (n = 1,000 HJ molecules).

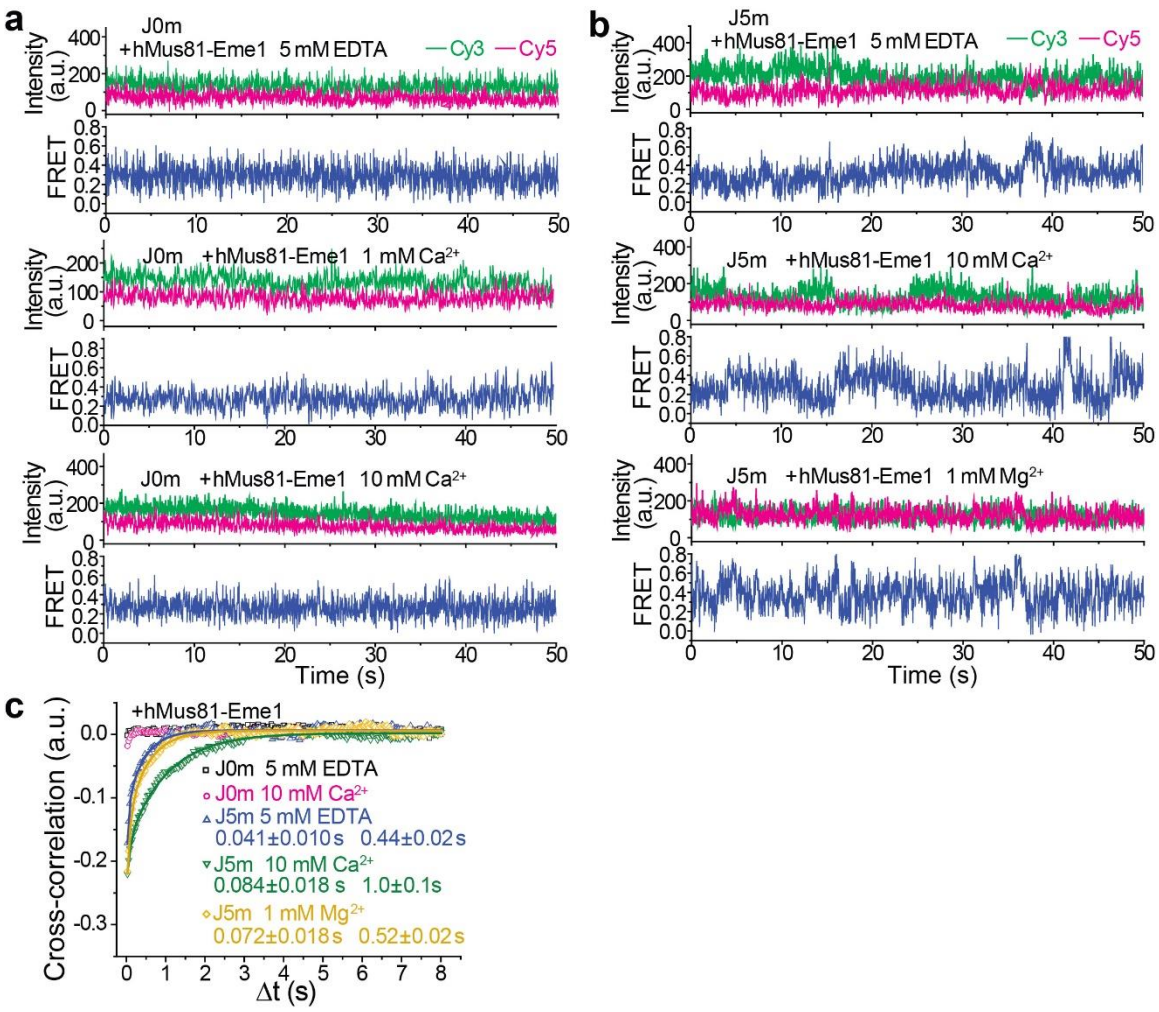

Supplementary Figure 17: hMus81-Eme1 binding to J5m permits branch migration. **a,** Single molecule time traces of hMus81-Eme1-bound J0m obtained at 5 mM EDTA, 1 mM Ca^{2+} or 10 mM Ca^{2+}. Partial dissociation of hMus81-Eme1 was not clearly observed in the time traces, presumably because the E_{FRET} for the **PD** state was not distinguishable from that of the fully bound state. **b,** Single molecule time traces of hMus81-Eme1-bound J5m obtained at 5 mM EDTA, 10 mM Ca^{2+}, or 1 mM Mg^{2+}, showing branch migration induced E_{FRET} fluctuations. **c,** Time scales of E_{FRET} fluctuations shown in (**a**) and (**b**) were determined from cross-correlation analysis. The HJ dynamics can be described by a single time component without hMus81-Eme1 bound and by two time components with hMus81-Eme1 bound. Means ± s.e.m are indicated (n = 1,000 HJ molecules).

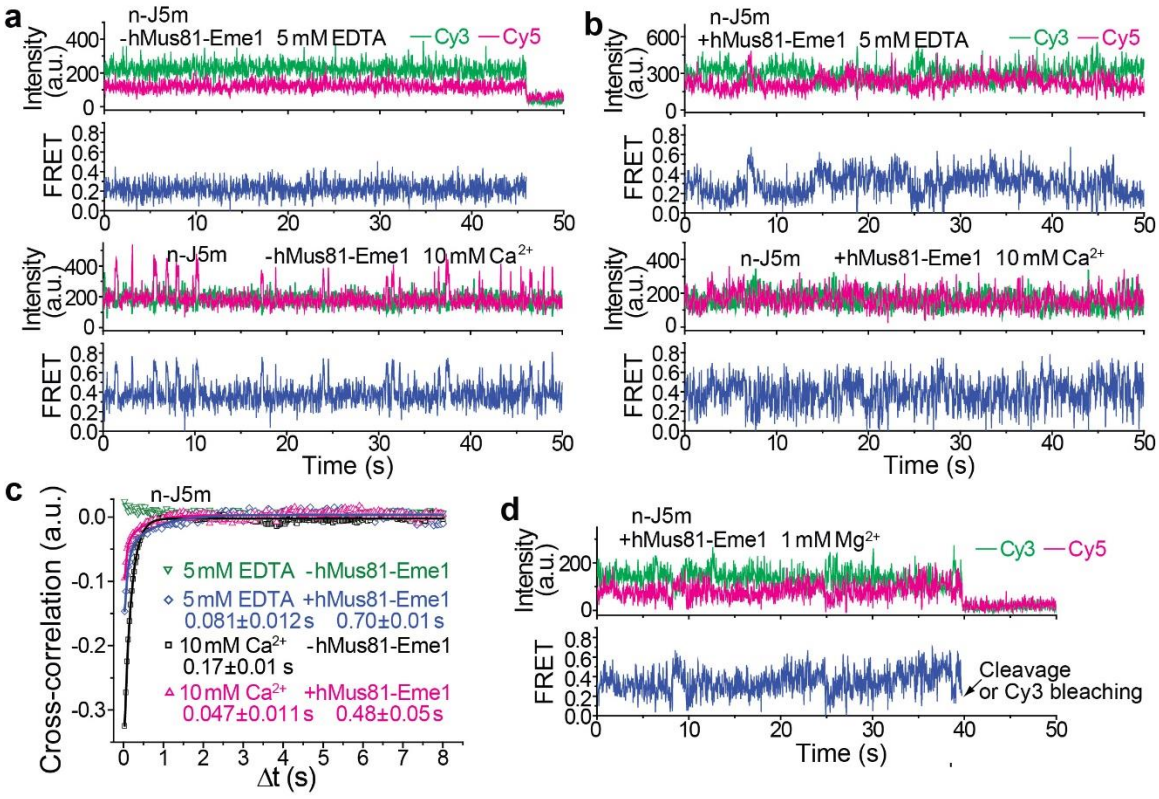

Supplementary Figure 18: hMus81-Eme1 binding to nicked J5m (n-J5m) permits branch migration. a, Single molecule time traces of bare n-J5m obtained at 5 mM EDTA or 10 mM Ca^{2+}. **b,** Single molecule time traces of hMus81-Eme1-bound n-J5m obtained at 5 mM EDTA or 10 mM Ca^{2++}, showing branch migration induced E_{FRET} fluctuations. **c,** Time scales of E_{FRET} fluctuations shown in **a, b-** were determined from cross-correlation analysis. The HJ dynamics can be described by a single time component without hMus81-Eme1 bound and two time components with hMus81-Eme1 bound. Means ± s.e.m are indicated (n = 1,000 HJ molecules). **d,** Single molecule time traces of hMus81-Eme1-bound n-J5m obtained at 1 mM Mg^{2+}, showing branch migration induced E_{FRET} fluctuations. The average cleavage rate is 2-5 min^{-1} as measured in the single molecule resolving enzyme cleavage assay (Supplementary Figure 1), which gave a sufficient observation time window to record the dynamics of hMus81-Eme1-bound n-J5m in Mg^{2+}.

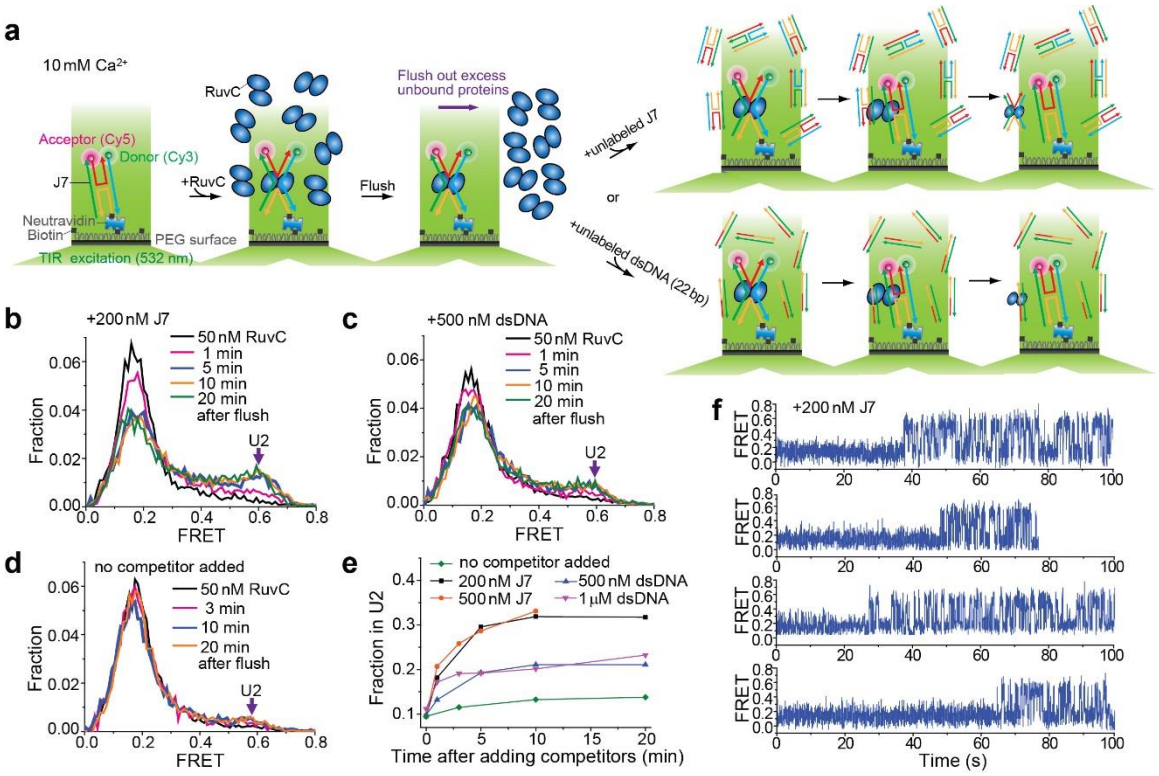

Supplementary Figure 19: Competition binding assay under single molecule conditions. a, Experimental scheme for the competition binding assay. 100 pM of Cy3/Cy5 labeled J7 were immobilized on the PEG surface. 50 nM RuvC were incubated with the tethered J7 for 5 min in 10 mM Ca^{2+} and excess unbound proteins were flushed out using buffer containing 10 mM Ca^{2+}. Unlabeled competitor DNA (J7 or 22-bp DNA duplex) was immediately introduced to the sample chamber. E_{FRET} histograms were obtained at different times after introducing the competitor DNA. **b,** E_{FRET} histograms were obtained at different time points after introducing 200 nM unlabeled J7. **c,** E_{FRET} histograms were obtained at different time points after introducing 1 μM unlabeled 22-bp double-stranded (ds)DNA. **d,** E_{FRET} histograms were obtained at different time points after flushing out the excess unbound RuvC, without adding any competitor DNA. **e,** Fraction of J7 in the **U2** state, estimated by accumulating the total fraction between 0.4 and 0.8 E_{FRET} , as a function of time. **f,** Representative smFRET-time traces of RuvC-bound J7 recorded immediately after adding the DNA competitor showing the complete dissociation of RuvC.

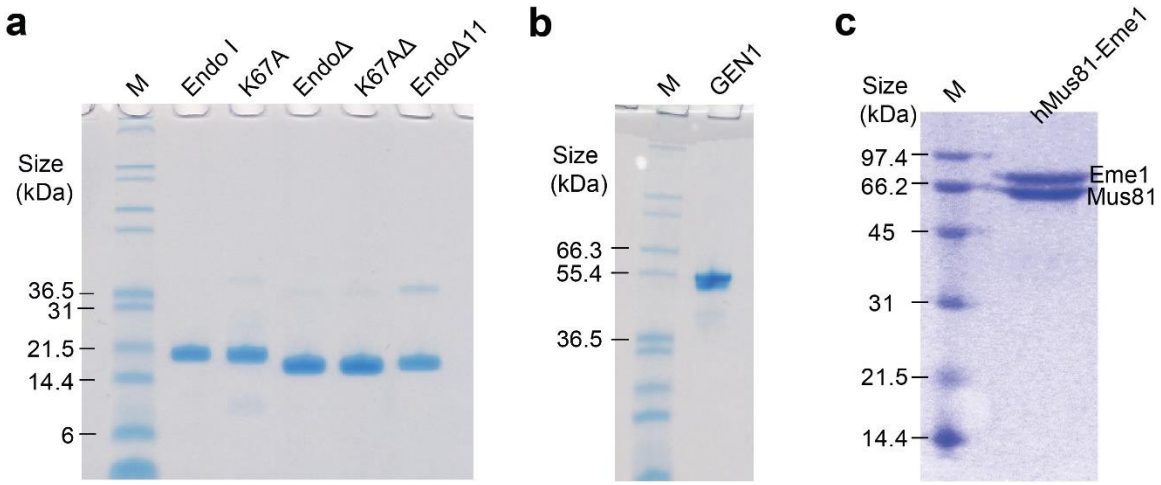

Supplementary Figure 20: Purity of Endo I, GEN1 and hMus81-Eme1. a, 12.5% SDS-PAGE showing the wild type Endo I and various Endo I mutants used in this study. Note that in each case the faint higher molecular weight band is a dimer of Endo I. **b,** 10% SDS-PAGE showing the GEN1 sample used in this study. **c,** 10% SDS-PAGE showing the full length hMus81-Eme1 used in this study. M is a molecular weight marker.